

## Ballistic-electron-emission microscopy of electron transport through AlAs/GaAs heterostructures

W. J. Kaiser, M. H. Hecht, L. D. Bell, and F. J. Grunthaler, and J. K. Liu

*Center for Space Microelectronics Technology, Jet Propulsion Laboratory, California Institute of Technology, Pasadena, California 91109*

L. C. Davis

*Research Staff, Ford Motor Company, Dearborn, Michigan 48121-2053*

(Received 10 September 1993)

BEEM spectroscopy has been used to characterize hot-carrier transport through AlAs/GaAs heterostructures. The dependence of electron transmission on AlAs thickness has been directly measured, and the position of the AlAs  $L_1$  minima, which has been subject to some uncertainty in the past, has been determined. First-principles transmission calculations, based on a tight-binding formalism, are compared to the results of BEEM spectroscopy.

The characterization of semiconductor heterostructures is an extremely active area of current experimental research. This strong interest is in large part motivated by the wealth of novel device applications developed over the last decade. There is a great deal of interest in the more fundamental aspects of interface formation and band alignments, and the desire for a unified description of interfaces has spawned many theories of interface formation, each of which demonstrates agreement with a greater or lesser fraction of the accumulated experimental results. From the point of view of device performance, the determination of transport through these structures is also of great importance.

The AlAs/GaAs material system, including the intermediate AlGaAs fractions, is the most studied family of heterostructures.<sup>1</sup> The capability for epitaxy in this system is highly developed, and a great deal of theoretical work has also been performed.<sup>2,3</sup> A precise experimental characterization, both of the AlAs/GaAs interface electronic structure and of transport characteristics in this system, is necessary for the development of a consistent theoretical description. For example, an uncertainty concerning the energies of the conduction-band minima within AlAs has not been resolved.<sup>4</sup>

Band offsets at semiconductor interfaces have conventionally been probed by using techniques such as internal photoemission and x-ray photoemission spectroscopy. Transport through heterostructures has been characterized primarily through current-voltage measurements on single- and double-barrier systems. In such two-terminal measurements, however, it is not possible to perform an energy spectroscopy of transport; in addition, the bending of the bands due to application of the voltage complicates analysis of the results. Three-terminal spectroscopy measurements have been performed<sup>5,6</sup> on macroscopic devices over a limited energy range.

This paper describes the microscopic characterization of the AlAs/GaAs interface by ballistic-electron-emission microscopy<sup>7</sup> (BEEM). BEEM is a technique, based on scanning tunneling microscopy<sup>8</sup> (STM), which utilizes the STM tip to inject ballistic carriers by vacuum tunneling into a heterostructure. The resulting forward-peaked dis-

tribution of carriers may then be used to perform a spectroscopy of transport through the sample structure. By measuring the fraction of the tunnel current which enters the semiconductor collector as a function of tunnel voltage, local properties of the interface such as barrier height, electronic band structure, and interface transmission efficiency may be probed directly. Interface imaging may also be performed with nanometer spatial resolution. This technique has previously been extensively applied to the Schottky-barrier interface with great success. In the present work, a detailed BEEM spectroscopy of electron transport through Au/AlAs/GaAs structure is presented, focusing on the development of band structure with AlAs thickness, and the corresponding effects on electron transport. The effectiveness of AlAs as a barrier to diffusion in the Au/GaAs system has already been demonstrated by BEEM characterization.<sup>9</sup>

A series of Au/AlAs/GaAs structures with different thicknesses of AlAs was fabricated by molecular-beam epitaxy (MBE). Substrate cleaning prior to MBE growth has been described previously.<sup>9</sup> The MBE procedure consisted of a growth of a 1- $\mu\text{m}$ -thick GaAs buffer layer ( $n = 5 \times 10^{16} \text{ cm}^{-3}$ , Si doped) on the  $n$ -GaAs(100) substrate ( $n = 3 \times 10^{16} \text{ cm}^{-3}$ , Si doped) under As-stabilized conditions, yielding the  $(2 \times 4)$  surface reconstruction as observed by reflection high-energy electron diffraction (RHEED). The sample was then annealed in the As flux to promote surface smoothing. The AlAs layer was deposited under RHEED control; monitoring of the RHEED oscillations provided precise control of AlAs thickness. The sample was transferred under UHV to the Au deposition chamber for completion by evaporation of 100 Å of Au. Electron transport through these structures was characterized by BEEM spectroscopy in a nitrogen-gas-purged glove box at room temperature. BEEM spectra of collector current  $I_c$  versus tunnel voltage  $V$  were acquired at a constant tunnel current of 1 nA. Samples with four different thicknesses of AlAs were analyzed. A qualitative energy diagram for these sample structures is shown in Fig. 1.

The derivatives  $dI_c/dV$  of representative BEEM spectra for the four samples are plotted as a function of  $V$  in

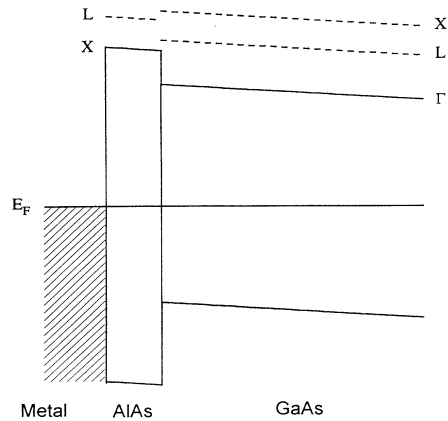


FIG. 1. Schematic energy diagram for a metal/AlAs/GaAs system.

Fig. 2. Differentiation of the  $I_c$ - $V$  data makes the multiple threshold nature of the data more apparent. The "0 monolayer (ML)" derivative designates a sample with no AlAs interlayer between the Au and the GaAs. Within the phase-space model which has been used previously to interpret BEEM spectroscopy results, the two limiting case spectra, representing Au/GaAs and Au/AlAs, may be interpreted. BEEM of Au/GaAs has already been characterized.<sup>7,10,9</sup> The position of the first threshold represents the Schottky-barrier height (SBH). In GaAs, a direct semiconductor, this is defined by the  $\Gamma_1$  point at the interface and occurs at 0.89 V. A second threshold is encountered at 1.18 V, which is produced by the onset of propagation into the  $L_1$  minima of GaAs. A weaker third threshold, at the onset of  $X_1$ -minima transmission, also occurs at higher voltage.

The sample with the thickest (50 ML) layer of AlAs ensured that the interlayer was opaque to electrons with energies less than the AlAs conduction-band minimum, and was therefore representative of transport in Au/AlAs.

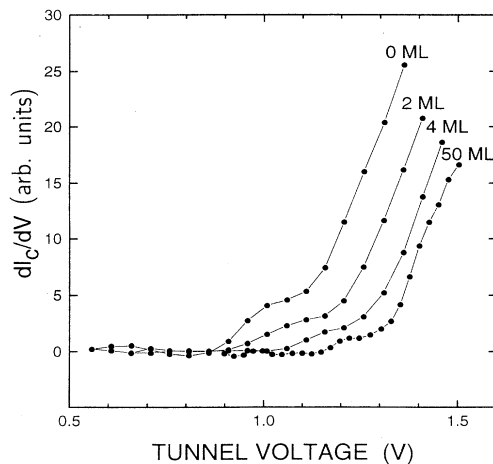


FIG. 2. Derivatives  $dI_c/dV$  for BEEM spectra of Au/AlAs/GaAs structures. Data are shown for AlAs thicknesses of 2, 4, and 50 ML. Also shown is a derivative spectrum for Au/GaAs (labeled "0 ML").

The Au/AlAs spectrum reflects features of the AlAs band structure. An initial threshold is observed at 1.15 V, which agrees well with previous measurements of the SBH for this system.<sup>11</sup> In AlAs, this is defined by conduction-band minima along the  $\Gamma_1$ - $X_1$  directions. A second threshold at 1.35 V also appears in the derivative. This threshold determines the  $L_1$ -minima energy in AlAs. The location of this band has been the subject of some controversy, but appears unambiguously here. Previous measurements have relied on extrapolations of  $\text{Al}_x\text{Ga}_{1-x}\text{As}$  data, with experimental measurements only to  $x=0.6$ .<sup>4</sup> Casey and Panish<sup>12</sup> provided an estimate of  $E_L-E_X$  between 0.08 and 0.18 eV. Lee *et al.*<sup>13</sup> give  $E_L-E_X=0.2$  eV from extrapolation of electrical measurements. Godby, Schluter, and Sham<sup>4</sup> tabulate experimental values indicating a  $E_L-E_X$  range from 0.25 to 0.30 eV. The value from BEEM of 0.2 eV agrees well with previous extrapolations. The  $\Gamma_1$  point should occur at approximately 2.0 V and is beyond the range of the data.

BEEM transport spectra representing intermediate thicknesses of AlAs reveal both GaAs and AlAs electronic structure and are less straightforward to interpret. The band structure of the thinnest AlAs layers is not yet bulklike; in addition, the presence of electron tunneling and standing waves in the AlAs layer must be treated. Of primary importance is an understanding of the attenuation of GaAs substrate contributions as AlAs thickness increases. In order to provide insight into the qualitative features of electron transport in these structures, transmission probabilities were calculated using the reduced Hamiltonian method of Schulman and Chang.<sup>14</sup> Since the structure of the Au film deposited on the semiconductor surface is not well defined, we have chosen instead (for computational convenience) to consider structures where the Au is replaced by a material such as  $\alpha$ -Sn that has the same structure as the underlying semiconductor and can be described straightforwardly within the method of Ref. 14. Au, on the other hand, is difficult to treat with this formalism. Since  $\alpha$ -Sn is metallic, it may provide qualitative understanding of experimental data. In our calculations,  $k_{\parallel}$  is conserved; thus some thresholds (such as  $L_1$  in GaAs) will not appear. The breakdown of  $k_{\parallel}$  conservation by scattering is required to detect such thresholds. The choice of metal has no effect on  $k_{\parallel}$  conservation, which depends only on the presence or lack of scattering. Since the details of the scattering are uncertain,<sup>15</sup> a scattering contribution is not included in the model.

This method is based upon a tight-binding description of the energy bands and wave functions and is exact within that description. We specialize the method to a (100) interface and use the  $sp^3s^*$  tight-binding model of Vogl, Hjalmanson, and Dow.<sup>16</sup> Some simplification results because interactions extend only to the nearest neighbors and spin-orbit coupling is neglected. Although the model has limitations, it nonetheless can provide an adequate qualitative picture of the interface. A more accurate description might be given by the method of Ando and Akera,<sup>17</sup> who used a combination of tight binding for the boundary conditions and effective-mass approximations for the bands. Stiles and Hamann<sup>18</sup> have also ap-

plied the method of linearized augmented plane waves to epitaxial interfaces. Such studies are, however, beyond the scope of the present work. Fortunately, many of the features of the BEEM spectra depend only on energy levels and  $\mathbf{k}$  vectors, which the tight-binding model reproduces with sufficient accuracy.

This theory has been applied to a series of calculations of the total transmission probability  $D$  for  $\alpha$ -Sn/AlAs/GaAs. Only normal incidence ( $\mathbf{k}_{\parallel}=0$ ) is considered, and in the energy range shown only one band in  $\alpha$ -Sn propagates, namely a band extending from  $\Gamma_{15}$  at  $k_z=0$  to  $X_5$  at  $k_z=2\pi/a$  (Fig. 11 of Vogl, Hjalmarson, and Dow). All energies are referred to the GaAs valence-band maximum. The AlAs valence band is offset from GaAs by 0.47 eV (Ref. 17) in the tight-binding calculation, so all diagonal energies of AlAs have been decreased by this amount. The  $\alpha$ -Sn parameters are left unchanged. In Fig. 3, we show results for  $\alpha$ -Sn/GaAs and three thicknesses of AlAs. Each plot is labeled by the number of ML's of AlAs. Also indicated are the levels used in the tight-binding calculation. In the following discussion, note that energies for the calculations in Fig. 3 are given in eV, relative to the GaAs VBM, whereas experimentally measured thresholds are given in V, relative to  $E_F$ . Both scales are shown in Fig. 3. The  $\Gamma_1$  threshold of GaAs is at 1.55 eV,  $X_1$  at 2.03 eV, and  $X_3$  at 2.38 eV. In AlAs,  $X_1$  is at 1.83 eV and  $X_3$  at 2.21 eV. The minimum energy is along  $\Delta$ , near  $X_1$ , at 1.80 eV, whereas  $\Gamma_1$  is much higher at 2.57 eV and is not encountered in these calculations.

The transmission probability for the  $\alpha$ -Sn/GaAs interface clearly shows the thresholds at  $\Gamma_1$  and  $X_1$ , and to a lesser extent  $X_3$ . The  $L_1$  threshold is at 1.69 eV but does not appear in calculations for normal incidence on a (100) interface, because transverse momentum ( $\mathbf{k}_{\perp}$ ) is conserved. On the other hand, both the  $\Gamma_1$  conduction band and the  $X_1$  valley in the [100] direction are final states allowed by transverse momentum conservation.

When there is an AlAs barrier, the transmission is considerably different. Below the  $\Delta$  threshold at 1.80 eV, the electron must tunnel through the AlAs to reach the  $\Gamma_1$  conduction band of GaAs. As a consequence, the probability  $D$  in this energy range decreases rapidly with thickness. This is reflected experimentally in the decay of the  $\Gamma$  threshold intensity in the data shown in Fig. 2. Over most of the range, our calculations show that the extinction constant  $\kappa$  is  $0.16(2\pi/a)(D \sim e^{-2\kappa d})$ , which is close to  $\text{Im}(k_z)$  for the  $\Gamma_1$  band [ $\approx 0.17(2\pi/a)$ ]. A plot of  $\text{Im}(k_z)$  has been given by Schulman and Chang (Fig. 1),<sup>20</sup> which is quite similar to our results. Tunneling via the  $\Delta$  minimum (or  $X_1$  valley) is less likely than via  $\Gamma_1$  since  $\text{Im}(k_z)$  for  $\Delta$  is actually larger for  $E < 1.69$  eV and the coupling of AlAs  $X_1$  valley states to GaAs  $\Gamma_1$  is weak over the entire energy range. For the 4-ML barrier, the calculation shows the presence of virtual standing waves in the AlAs  $X_1$  valley below the  $X_1$  edge in GaAs. Since the coupling to  $\Gamma_1$  is weak and there is some reflection at the  $\alpha$ -Sn interface, standing-wave resonances can be set up. Ando and Akeru have discussed this phenomenon in AlGaAs heterojunctions where the location of bands in

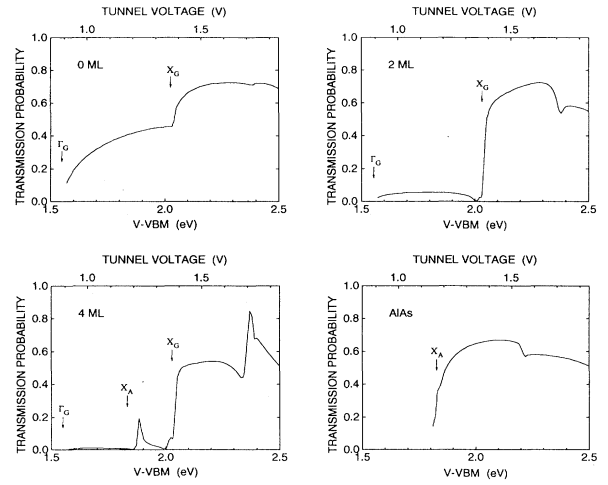


FIG. 3. One-dimensional transmission calculated for  $\alpha$ -Sn/GaAs,  $\alpha$ -Sn/AlAs/GaAs for AlAs thicknesses of 2 and 4 ML, and  $\alpha$ -Sn/AlAs. Also indicated are the tight-binding values for conduction-band minima  $\Gamma_1$  and  $X_1$  in GaAs and  $X_1$  in AlAs.

the barrier have the same ordering as here. However, as discussed below, these resonances do not appear directly in the BEEM spectrum.

Although transport via the  $L_1$  minima is not treated in the calculation, the qualitative features are similar. Since the  $L_1$  minima in GaAs lie at lower energy than in AlAs, the presence of the AlAs layer will produce a tunnel barrier for  $L_1$  transport. This will cause an attenuation of the intensity of the GaAs  $L_1$  threshold in the BEEM spectra. An additional threshold will also start to appear at higher energy, at the  $L_1$  minima in AlAs. Electron transport in this case will not involve either  $\Gamma_1$  or  $X_1$  in either material, due to  $\mathbf{k}_{\parallel}$  conservation.

Above the  $X_1$  threshold of GaAs, the probability of transmission is large,  $\approx 0.8$ , indicating that the electron is propagating through the AlAs via the  $X_1$  valley, where it is strongly coupled to the  $X_1$  states in GaAs. Observation of the onset of  $X_1$ - $X_1$  transmission in the data, however, will be complicated by the presence of  $L_1$ - $L_1$  transmission, which should also produce a strong threshold. Since  $L_1$  in AlAs (1.35 V) lies near in energy to  $X_1$  in GaAs (1.38 V), these two transport processes will onset at approximately the same voltage.

When the thickness of the barrier exceeds the mean free path, a different behavior is observed in the calculated transmission that does not show the threshold of the GaAs, but only AlAs electronic structure. As shown in Fig. 3, the  $X_1$  and  $X_3$  thresholds of AlAs appear; again, the  $L_1$  threshold does not appear in these one-dimensional calculations due to conservation of  $\mathbf{k}_{\parallel}$ , although it is clearly seen in the data.

In a BEEM experiment, the  $\Gamma_1$ ,  $L_1$ , and  $X_1$  thresholds will have the usual  $(V - V_b)^2$  dependence even in the presence of the AlAs barrier. The  $\Gamma_1$  current will be greatly reduced as the barrier thickness is increased, while the  $X_1$  should remain roughly the same. The

standing waves in the AlAs  $X_1$  valley will show a slightly different threshold behavior in  $I_c$ . In the one-dimensional case, we can replace a standing wave, or closely spaced group of waves, with a threshold  $V_{t1}$  where the current is turned on and a second threshold  $V_{t2}$  slightly above  $V_{t1}$  where the negative of the current is turned on. The difference between  $V_{t2}$  and  $V_{t1}$  is an effective width of the resonance. The collector current would then be of the form

$$I_c \sim f(V - V_{t1}) - f(V - V_{t2}),$$

where  $f(V - V_t)$  is the usual functional form of the BEEM collector current. However, the large spread in  $\mathbf{k}_{\parallel}$  in the three-dimensional case will broaden this threshold behavior from a steplike feature into a more gradual linear form,<sup>21</sup> which in the derivative will in turn appear as a step. This threshold is therefore not expected to exhibit the strong resonances which appear in the calculation, but rather should resemble the standard steplike BEEM threshold in the derivative. The first threshold in the 4-ML spectrum may owe some of its intensity to this resonant transport, since  $X_1$ - $X_1$  transport is not expected

until the  $X_1$  threshold in GaAs is reached at 1.38 V. A contribution below the AlAs  $X_1$  also appears to be present, indicating that tunneling through the AlAs gap into  $\Gamma_1$  of GaAs is still appreciable.

In conclusion, BEEM has been used to investigate transport through AlAs/GaAs semiconductor heterostructures. The dependence of transport on AlAs thickness has been directly measured. For the case of Au on thick AlAs, the position of the  $L_1$  minima, which has been subject to some uncertainty in the past, has been directly determined. Results of BEEM spectroscopy have been compared to first-principles transmission calculations for equivalent thicknesses of AlAs on GaAs.

The research described in this paper was performed by the Center for Space Microelectronics Technology, Jet Propulsion Laboratory, California Institute of Technology, and was jointly sponsored by the Office of Naval Research and the Ballistic Missile Defense Organization/Innovative Science and Technology Office through an agreement with the National Aeronautics and Space Administration (NASA).

- 
- <sup>1</sup>S. Adachi, *J. Appl. Phys.* **58**, R1 (1985).  
<sup>2</sup>J. R. Chelikowsky and M. L. Cohen, *Phys. Rev. B* **14**, 556 (1976).  
<sup>3</sup>G. B. Bachelet and N. E. Christensen, *Phys. Rev. B* **31**, 879 (1985).  
<sup>4</sup>R. W. Godby, M. Schluter, and L. J. Sham, *Phys. Rev. B* **35**, 4170 (1987).  
<sup>5</sup>J. R. Hayes, A. F. J. Levi, and W. Wiegmann, *Phys. Rev. Lett.* **54**, 1570 (1985).  
<sup>6</sup>M. Heiblum, M. I. Nathan, D. C. Thomas, and C. M. Knoedler, *Phys. Rev. Lett.* **55**, 2200 (1985); M. Heiblum, E. Calleja, I. M. Anderson, W. P. Dumke, C. M. Knoedler, and L. Osterling, *ibid.* **56**, 2854 (1986).  
<sup>7</sup>W. J. Kaiser and L. D. Bell, *Phys. Rev. Lett.* **60**, 1406 (1988). For a more complete review of BEEM, see L. D. Bell, W. J. Kaiser, M. H. Hecht, and L. C. Davis, in *Scanning Tunneling Microscopy*, edited by J. A. Stroscio and W. J. Kaiser (Academic, San Diego, 1993), pp. 307–348.  
<sup>8</sup>G. Binnig, H. Rohrer, Ch. Gerber, and E. Weibel, *Phys. Rev. Lett.* **49**, 57 (1982).  
<sup>9</sup>M. H. Hecht, L. D. Bell, W. J. Kaiser, and F. J. Grunthaner, *Appl. Phys. Lett.* **55**, 780 (1989).  
<sup>10</sup>L. D. Bell and W. J. Kaiser, *Phys. Rev. Lett.* **61**, 2368 (1988).  
<sup>11</sup>S. M. Sze, *Physics of Semiconductors Devices*, 2nd ed. (Wiley, New York, 1981), p. 291.  
<sup>12</sup>H. C. Casey, Jr. and M. B. Panish, *Heterostructure Lasers* (Academic, New York, 1978), Pt. A, p. 191.  
<sup>13</sup>H. J. Lee, L. Y. Juravel, J. C. Woolley, and A. J. SpringThorpe, *Phys. Rev. B* **21**, 659 (1980).  
<sup>14</sup>J. N. Schulman and Y.-C. Chang, *Phys. Rev. B* **27**, 2346 (1983).  
<sup>15</sup>A. M. Milliken, S. J. Manion, W. J. Kaiser, L. D. Bell, and M. H. Hecht, *Phys. Rev. B* **46**, 12 826 (1992).  
<sup>16</sup>P. Vogl, H. P. Hjalmarson, and J. D. Dow, *J. Phys. Chem. Solids* **44**, 365 (1983).  
<sup>17</sup>T. Ando and H. Akera, *Phys. Rev. B* **40**, 11 619 (1989).  
<sup>18</sup>M. D. Stiles and D. R. Hamann, *Phys. Rev. B* **38**, 2021 (1988).  
<sup>19</sup>W. I. Wang and F. Stern, *J. Vac. Sci. Technol. B* **3**, 1280 (1985).  
<sup>20</sup>J. N. Schulman and Y.-C. Chang, *Phys. Rev. B* **31**, 2056 (1985).  
<sup>21</sup>G. N. Henderson, T. K. Gaylord, E. N. Glytsis, P. N. First, and W. J. Kaiser, *Solid State Commun.* **80**, 591 (1991).